Correction of the NMR structure of the ETS1/DNA complex

Milton H. Werner[a],*, G. Marius Clore[a],**, Constance L. Fisher[b], Robert J. Fisher[b],
Loc Trinh[c], Joseph Shiloach[c] and Angela M. Gronenborn[a],**

[a]*Laboratory of Chemical Physics, Building 5, NIDDKD, National Institutes of Health, Bethesda, MD 20892-0520, U.S.A.*
[b]*Frederick Cancer Research and Development Center, National Cancer Institute, Frederick, MD 21707, U.S.A.*
[c]*Laboratory of Cellular and Developmental Biology, NIDDKD, Bethesda, MD 20895-0520, U.S.A.*

Summary

The ETS family of transcription factors consists of a group of proteins that share a highly conserved 85 amino acid DNA-binding domain (DBD). This family recognizes a consensus sequence rich in purine bases with a central GGAA motif. A comparison of the published three-dimensional structures of the DBD/DNA complexes of ETS1 by NMR [Werner et al. (1995) *Cell*, **83**, 761–771] and the related Pu.1 by X-ray crystallography [Kodandapani et al. (1996) *Nature*, **380**, 456–460] reveals an apparent discrepancy in which the protein domains bind with opposite polarity to their target sequences. This surprising and highly unlikely result prompted us to reexamine our NMR structure. Additional NMR experiments now reveal an error in the original interpretation of the spectra defining the orientation of the ETS1-DBD on DNA. It was originally reported that the ETS1-DBD bound to DNA with a bipartite motif involving major groove recognition via a helix–turn–helix element and minor groove recognition via protein side-chain intercalation. The presence of intercalation was deduced on the basis of numerous NOEs between several amino acids in the protein and a resonance at 12.33 ppm originally assigned to a DNA imino proton. New NMR experiments now conclusively demonstrate that this resonance, which is located within the DNA imino proton region of the spectrum, arises from the hydroxyl proton of Tyr[86]. Realization of this error necessitated reanalysis of the intermolecular NOEs. This revealed that the orientation of the ETS1-DBD in the complex is opposite to that originally reported and that a tryptophan residue does not intercalate into the DNA. The calculation of a new ensemble of structures based on the corrected data indicates that the structure of the ETS1-DBD/DNA complex is indeed similar to the X-ray structure of the Pu.1-DBD/DNA complex.

Introduction

The ETS family of transcription factors is characterized by a highly conserved 85 amino acid DNA-binding domain (Wasylyk et al., 1993). The canonical member of this family, the human ETS1 oncoprotein, is a lymphocyte-specific regulator of gene expression that is involved in T-cell development and B-cell and T-cell maturation (MacLeod et al., 1992). Dysregulation of genes under the control of ETS proteins results in myeloid and erythroid leukemia in chickens, mice and humans (Hromas and Klemsz, 1994).

The 3D structures of the DNA-binding domain (DBD) of several ETS family members have been determined by NMR spectroscopy and X-ray crystallography in both the presence and absence of DNA. The DBD structures of mouse ETS1 (Donaldson et al., 1994,1996), human Fli-1 (Liang et al., 1994a,b), human ETS1 (Werner et al., 1995b) and mouse Pu.1 (Kodandapani et al., 1996) reveal an overall fold that is very similar to that of the DBD of the *E. coli* catabolite gene activator protein (CAP), namely an N-terminal α-helix, a four-stranded β-sheet and a helix–turn–helix (HTH) major groove recognition motif. We originally reported that the 3D NMR structure of the

human ETS1-DBD bound to a 17 base pair (bp) oligonucleotide duplex with complete intercalation of a single, highly conserved tryptophan residue (Trp[28]) at a CpC step 5' to the central GGAA motif (Werner et al., 1995b). In stark contrast, the X-ray structure of the DBD of a distant ETS family member, namely mouse Pu.1 in which Trp[28] is replaced by a Tyr, does not display intercalation and is oriented on the DNA with opposite polarity relative to that of our reported structure for the ETS1-DBD/DNA complex (Kodandapani et al., 1996).

Protein side-chain intercalation into DNA can be identified spectroscopically from the observation of numerous NOEs between side-chain protons of the protein and one or more base-paired imino protons of the DNA (King and Weiss, 1993; Werner et al., 1995a). We originally reported that Gln[26], Leu[27] and Trp[28] displayed several NOEs to a single guanine imino proton of the DNA (Werner et al., 1995b). New NMR experiments reported here, however, reveal that the resonance of this presumptive imino proton actually arises from the hydroxyl proton of Tyr[86]. Tyr[86]-**OH** in the ETS1-DBD/DNA complex resonates in the DNA imino proton region of the spectrum at a frequency (12.33 ppm) more than 2 ppm downfield from several previously reported positions for this infrequently observed resonance (Kraulis et al., 1989; Torchia et al., 1989; Liepinsh et al., 1992), although more recently there have been three reports of the observation of a putative tyrosine hydroxyl resonance downfield of 11 ppm (Pjura et al., 1993; Plesniak et al., 1996; Zhao et al., 1996). The chemical shift of the resonance at 12.33 ppm was the most significant factor leading to its misinterpretation. This error in spectroscopic analysis, coupled with numerous misassignments of interfacial NOEs derived therefrom, resulted in the improper positioning of the ETS1-DBD on DNA. Correction of the misassignment and a subsequent reanalysis of the intermolecular NOEs were followed by the calculation of a new solution NMR structure for the ETS1-DBD/DNA complex. This structure is similar to the X-ray structure of the Pu.1-DBD/DNA complex (Kodandapani et al., 1996). A brief erratum to this effect has been published where the original report appeared (Werner et al., 1996a), and the corrected coordinates deposited in the Brookhaven Protein Databank. In this paper we present a more detailed description and analysis of this error and the corrected structure of the complex. We note that the incorrect ETS1-DBD/DNA complex was included in a review dealing with proteins that bend DNA by intercalating in the minor groove (Werner et al., 1996b). While ETS1 clearly no longer belongs to this class of DNA binding proteins, the hypothesis and conclusions presented in the review are unaffected, and indeed are only further strengthened by recent crystallographic results on complexes of integration host factor (Rice et al., 1996) and the Lac repressor (Lewis et al.,

1996) with DNA, both of which reveal minor groove intercalation by a hydrophobic residue.

Materials and Methods

Sample preparation

The ETS1-DBD used in the present study comprises residues 311–415 of the p51 isoform of the ETS1 protein (Fisher et al., 1991). An additional 25 amino acids (MGS-SHHHHHHSSGLVPRGSHMLEDL) were added onto the N-terminus for purification purposes as a histidine tag using the modified pET15b (Novagen) vector SBpET+1 (Fisher et al., 1994). In this paper, the first arginine of the ETS1 sequence (residue 311) is numbered as residue 1. The ETS1-DBD, uniformly (>98%) labeled with either ^{15}N or ^{13}C and ^{15}N, was expressed in minimal medium using ^{15}NH$_4$Cl and/or ^{13}C$_6$-glucose as the sole nitrogen and carbon sources, respectively, and purified as described previously (Fisher et al., 1991) with minor modifications. The DNA strands were synthesized and purified as described previously (Werner et al., 1995b).

The complex was formed by two different methods that led to indistinguishable NMR spectra. The first method mixed denatured protein (8–15 mg/ml) in 6 M guanidine hydrochloride, 50 mM Tris, 50 mM dithiothreitol (DTT), pH 7.5, with 1.05 equiv (mol/mol) duplex DNA at room temperature and the entire solution refolded by gel-filtration chromatography as previously described (Werner et al., 1994,1995b). In the second method, the protein (8–15 mg/ml) was denatured in 50 mM Tris, 6 M guanidine-hydrochloride, 50 mM DTT, pH 8.0. The denatured, reduced protein was then rapidly diluted into a solution containing 10 mM sodium phosphate, 35 mM sodium chloride, 2 mM DTT and 1.05 equiv (mol/mol) duplex DNA; the protein concentration after dilution varied from 0.2 to 0.3 mg/ml and the final guanidine concentration varied from 0.15 to 0.3 M. The protein/DNA complex from either method was then concentrated in a Centriprep-10 (Amicon) and/or by vacuum dialysis (Micro-ProDiCon, Spectrum), and dialyzed such that the samples used for the NMR experiments contained 1.1 mM ETS1-DBD, 1.17 mM duplex DNA 17-mer, 5 mM imidazole, 5 mM NaN$_3$, 50 μM Na$_2$-EDTA, 2 mM DTT, pH 6.8, in either degassed 100% D$_2$O or degassed 95% H$_2$O/5% D$_2$O. Subsequent to concentration, residues of the histidine tag were cleaved in the NMR samples with human thrombin (4–8 units/10 mg ETS1-DBD protein) for 6 h at room temperature. The enzyme was removed by the addition of 20 μl benzamidine-sepharose (Pharmacia) with mixing for 1 h. The sepharose was removed by centrifugation and the supernatant was used for NMR studies without removal of the cleaved peptide. The cleaved peptide was not removed as cleavage was conducted under conditions used for the NMR experiments in order to avoid further sample loss by additional manipulations. Resonances for

the backbone and side-chain resonances of the cleaved peptide could be identified on account of their narrow line widths. No NOEs between the amino acids of the cleaved peptide and the ETS1-DBD were observed. No additional cleavage of the sample could be discerned by denaturing electrophoresis even after 6 months. The proportion of free DNA in the samples was determined by capillary zone electrophoresis and NMR spectroscopy, and did not exceed 5%. The DNA binding activity of the protein domain prepared by both methods was assessed by electrophoretic mobility shift (data not shown). The

protein refolded by rapid dilution and cleavage had the same specificity and affinity for DNA as the uncleaved protein prepared by chromatographic refolding. More than 80% of the data collected were obtained from samples prepared with the rapid-dilution method of refolding, including all of the data for sequential assignment of the DNA and analysis of intermolecular contacts.

NMR spectroscopy and structure calculations

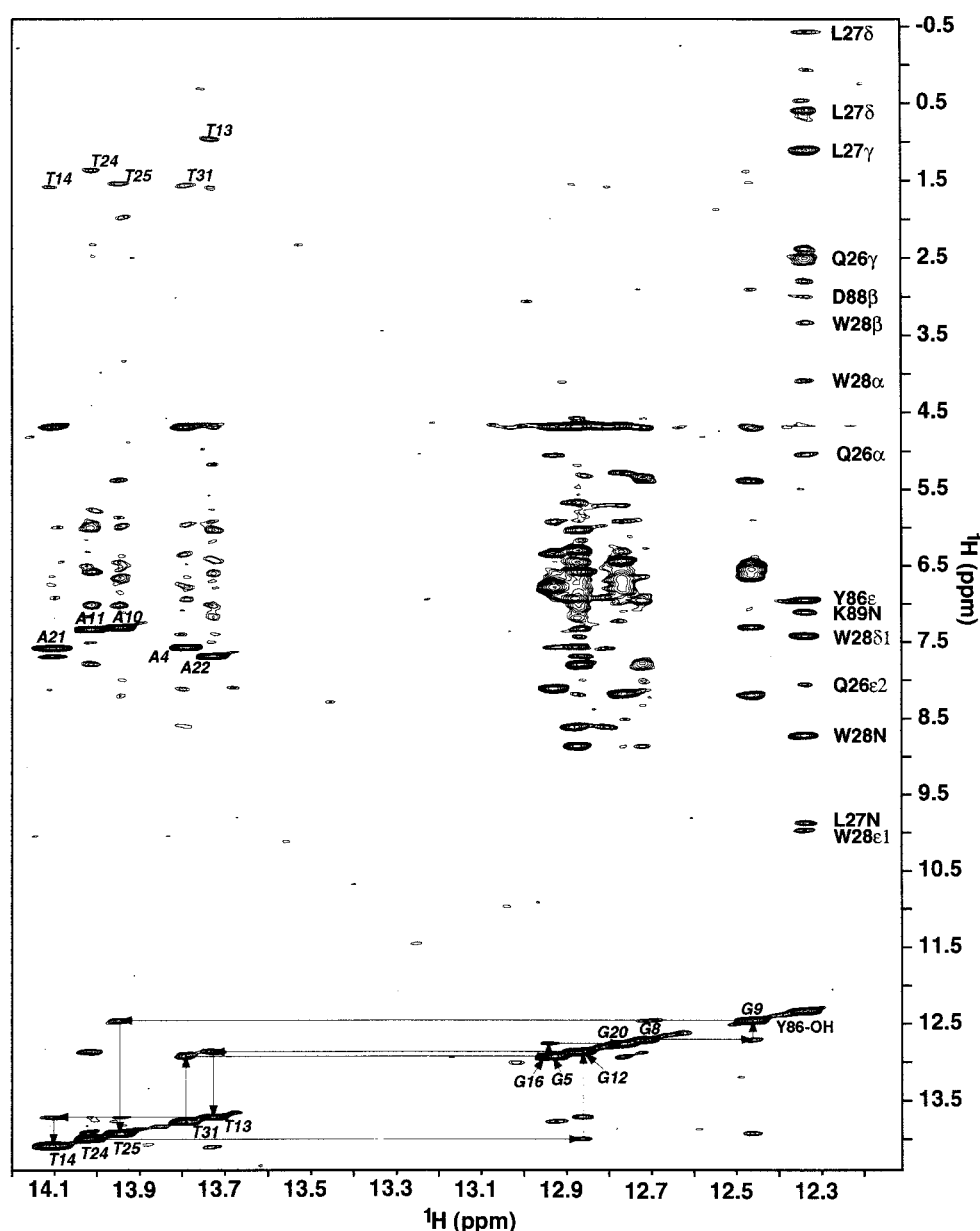All NMR experiments were carried out at 32 °C on either Bruker AMX500 or AMX600 spectrometers equip-

Fig. 1. A portion of the ^{1}H-^{1}H NOE spectrum (155 ms mixing time) of the ETS1-DBD/DNA complex recorded in H$_2$O, illustrating NOEs to DNA imino protons and the hydroxyl proton of Tyr[86]. Sequential connectivities between DNA imino proton resonances are indicated by vertical and horizontal lines. The assignments of the DNA imino proton resonances on the diagonal and the intra-base-pair NOE cross peaks involving the adenine H2 and the thymine methyl protons are indicated in italics. The Tyr[86] hydroxyl proton appears just upfield of the imino proton of G9 and the assignments of cross peaks arising from the protein backbone and side-chain atoms near this hydroxyl proton are indicated.

ped with a z-shielded gradient triple-resonance probe. Details of the assignment of protein, DNA and determination of the 3D structure have been previously described (Werner et al., 1995b). For reference, the aromatic resonances in the original paper (Werner et al., 1995b) were assigned using the combined information from 2D ^{1}H-^{13}C HMQC, 2D ^{1}H-^{1}H HOHAHA, 2D ^{1}H-^{1}H NOE and 3D ^{13}C-edited NOE spectra.

A 3D ^{13}C-edited HMQC-NOESY experiment was recorded in H_2O with a jump-and-return water suppression sequence (Plateau and Guéron, 1982) on a freshly prepared sample at 500 MHz, 32 °C, pH 6.8. For the observation of the weak ^{3}J coupling of Tyr^{86}-OH to Tyr^{86}-C$^\epsilon$, a 1D heteronuclear spin-echo difference experiment (Blake et al., 1992) was performed using the following pulse sequence:

$$^1\text{H:} \quad 90^\circ_{\phi 1} - \tau_1 - 90^\circ_{\phi 2} - \tau_2 - 90^\circ_x - \tau_3 | \tau_3 - 90^\circ_{\phi 3} - \tau_2 - \text{Acquire}$$

$$^{13}\text{C:} \quad\quad\quad\quad\quad\quad\quad 180^\circ_x$$

$$\text{PFG:} \quad\quad\quad G1 \quad\quad\quad\quad G1$$

where phases $\phi_1 = 2(x), 2(y), 2(-x), 2(-y)$, $\phi_2 = -\phi_1$, $\phi_3 = -x$; $\tau_1 = 60$ μs in order to center the excitation profile at ±7.6 ppm from the center of the ^{1}H spectrum at 4.7 ppm; τ_3 was 60 μs less one-half the length of the 180° ^{13}C pulse. The echo delay $\tau_2 = 20$ ms was set equal to approximately one T_2 value to maximize the sensitivity of the measurement. The ^{13}C carrier frequency is switched from 120 to 400 ppm every eight scans. Gradients (PFG), 250 μs in length, are sine-bell shaped, 25 G/cm at the center. For obtaining a reference spectrum (^{13}C carrier at 400 ppm), the receiver phase is $2(x), 2(-y), 2(-x), 2(y)$. For the difference spectrum, the receiver phase is inverted every eight scans relative to the reference receiver phase, together with the change in ^{13}C offset frequency. For the reference spectrum, 1024 transients were collected with a sweep width of 30 ppm. For the difference spectrum, 76 800 transients were recorded with the same sweep width.

NMR spectra were processed using the NMRPipe software package (Delaglio et al., 1995), and analyzed using the programs PIPP, CAPP and STAPP (Garrett et al., 1991).

The structures were calculated by simulated annealing (Nilges et al., 1988) using the program XPLOR (Brünger, 1993) incorporating restraints for ^{3}J$_{HN\alpha}$ coupling constants (Garrett et al., 1994) and secondary ^{13}C chemical shifts (Kuszewski et al., 1995). Restraints involving any ambiguities in the assignment of NOEs involving the H4', H5' and H5" sugar protons, as well as those involving non-stereospecifically assigned methylene and methyl protons, were treated as $\Sigma(r^{-6})^{-1/6}$ sums (Nilges, 1993). The percentage of residues in the most favorable region of the Ramachandran plot (Morris et al., 1992) in the final simu-

lated annealing structures is ~75%. The coordinates of the 25 final simulated annealing structures of the ETS1-DBD/DNA complex, together with the coordinates of the restrained regularized mean structure, $(\overline{\text{SA}})$r, and the complete list of experimental NMR restraints and ^{1}H, ^{15}N, ^{13}C assignments have been deposited in the Brookhaven Protein Databank (accession numbers 2STT, 2STW and 2STWMR, respectively).

Results

NMR spectroscopy and assignment of the downfield shifted resonance of the hydroxyl proton of Tyr^{86}

In contrast to our previous report (Werner et al., 1995b), we show that intercalation of Trp^{28} into the DNA does not occur. Intercalation of a protein side chain must necessarily unstack the DNA bases, exposing the hydrogen-bonded imino protons to direct interaction with the protons of protein side chains (King and Weiss, 1993; Werner et al., 1995a,c). NOEs are therefore expected to be observed between two sequential imino protons of the DNA and protons of protein side chains. This diagnostic spectroscopic signature of intercalation was first observed in the complex of the human testis determining factor SRY bound to DNA (King and Weiss, 1993; Werner et al., 1995a,c), and subsequently in the complex of the lymphocyte specific protein LEF-1 bound to DNA (Love et al., 1995). Figure 1 illustrates that several NOEs occur between a proton at 12.33 ppm and the side-chain protons of Gln^{26}, Leu^{27} and Trp^{28} (as well as others). The chemical shift of this proton is consistent with that of a DNA imino proton (i.e. 12–14 ppm) and this resonance was originally assigned to the imino proton of G29 (Werner et al., 1995b). The only protein signals generally observed in this region of the proton NMR spectrum arise from either a downfield shifted tryptophan indole proton or a nitrogen-bonded hydrogen of a histidine ring. If the signal at 12.33 ppm, however, belonged to either of these amino acids, it would display an ~90 Hz coupling to a directly attached ^{15}N nucleus in a uniformly ^{15}N/^{13}C-enriched sample. No such coupling was observed for this proton nor was a coupling observed for this proton to a directly attached ^{13}C nucleus. In addition, the resonance at 12.33 ppm is not present in spectra of the DNA-free ETS1-DBD. On this basis, the resonance at 12.33 ppm was originally assumed to belong to a DNA imino proton. This immediately implied that side-chain intercalation should be present in the ETS1-DBD/DNA complex. The question was where this insertion into the DNA might occur.

The imino proton resonances of 12 of the 17 base pairs (specifically base pairs 2–5 and 8–16) were sequentially assigned in the ETS1-DBD/DNA complex on the basis of NOEs between neighboring imino protons and NOEs between the adenine H2 proton and the imino protons of
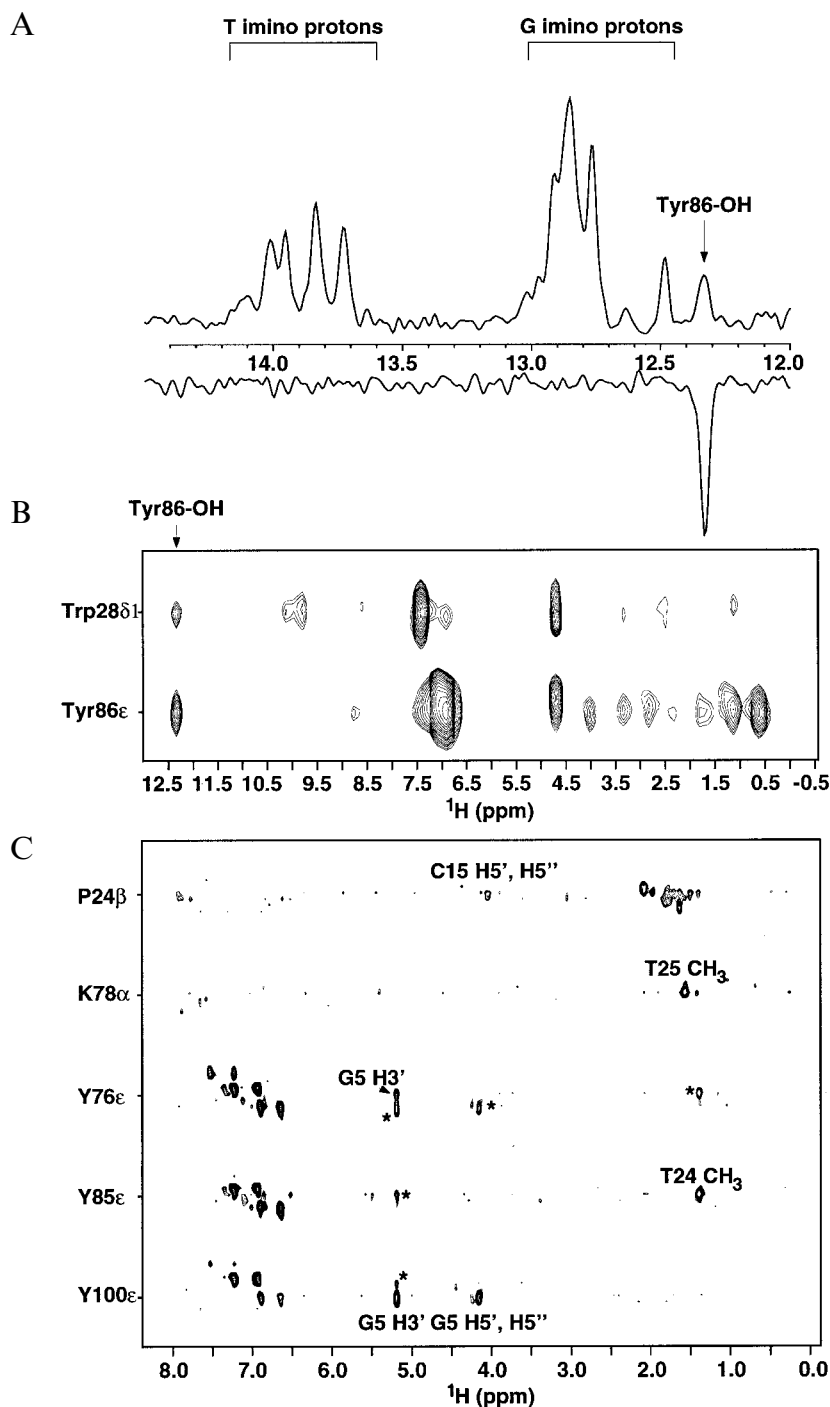
Fig. 2. Assignment of the Tyr[86] hydroxyl proton and intermolecular contacts defining the orientation of the ETS1-DBD on DNA. (A) 1D heteronuclear spin-echo difference spectrum recorded in H_2O, demonstrating that the resonance at 12.33 ppm is directly coupled to a ^{13}C nucleus. The top trace is the reference spectrum. The bottom trace is the difference spectrum collected with 75 times the number of scans collected for the reference spectrum. When the difference in the number of scans is taken into account, the difference spectrum is plotted at a scale approximately 16-fold greater than that of the reference spectrum. (B) Strips taken from the 3D ^{13}C-edited NOE spectrum (120 ms mixing time) recorded in H_2O, demonstrating the proximity of protons from Trp[28] and Tyr[86] to the signal at 12.33 ppm. (C) Strips taken from the 3D ^{13}C-edited/^{12}C-filtered NOE spectrum (100 ms mixing time), illustrating intermolecular NOEs between protein side chains and DNA. Asterisks indicate peaks from one amino acid appearing in the same strip as those from another amino acid as a consequence of the similarity of the [13]C[ε] chemical shifts for Tyr[76], Tyr[85] and Tyr[100]. In the original figure of the Y85ε strip presented in Fig. 1 of Werner et al. (1995b), the peak labeled T24 CH$_3$ in the current figure was identified as T25 (H2'); the ^{1}H shifts of these two DNA resonances are in fact degenerate, but in the current set of structures Y85ε was always less than 5 Å from T24 (CH$_3$) but greater than 10 Å away from T25 (H2'). This is due to the opposite orientation of binding in the incorrect and revised structures. The peak marked with an asterisk at 5.16 ppm in the present Y85ε strip was originally assigned to A22 (H3') (Werner et al., 1995b), but we have subsequently found that the resonance of A22 is actually located at 5.10 ppm. Even in the present structures, however, Y85ε is still only about 4.5 Å away from A22 (H3').

TABLE 1

INTERMOLECULAR NOEs OBSERVED IN THE 100 ms MIXING TIME 3D ^{13}C-SEPARATED/^{12}C-FILTERED NOE SPECTRUM OF THE ETS1-DBD/DNA COMPLEX RECORDED AT 600 MHz

Protein	DNA
Pro[24] (C$^\beta$H)	C15 (H5'/H5")
Leu[27] (C$^\delta$H$_3$)	C23 (H5'/H5")
Lys[69] (C$^\gamma$H)	T24 (H3')
Lys[69] (C$^\delta$H)	T24 (H3'), T24 (H5'/H5")
Lys[69] (C$^\epsilon$H)	T24 (H1'), T24 (H2'), T24 (H3'), T24 (H5'/H5")
Lys[71] (C$^\epsilon$H)	T25 (H3'), T25 (H6)
Met[74] (C$^\epsilon$H$_3$)	T25 (CH$_3$), T25 (H5'/H5")
Tyr[76] (C$^\epsilon$H)	G5 (H3')
Lys[78] (C$^\alpha$H)	T25 (CH$_3$)
Ser[80] (C$^\beta$H)	C7 (H4')
Arg[81] (C$^\beta$H)	T25 (H6)
Tyr[85] (C$^\delta$H)	T24 (CH$_3$)
Tyr[85] (C$^\epsilon$H)	C23 (H2'), T24 (CH$_3$)
Tyr[86] (C$^\epsilon$H)	C23 (H2')
Lys[89] (C$^\delta$H)	A22 (H4')
Lys[94] (C$^\delta$H)	C7 (H5'/H5")
Lys[94] (C$^\epsilon$H)	C7 (H3'), C7 (H5'/H5")
Arg[99] (C$^\delta$H)	G5 (H5'/H5") or C6 (H5'/H5")
Tyr[100] (C$^\delta$H)	G5 (H3')
Tyr[100] (C$^\epsilon$H)	G5 (H3'), G5 (H4'), G5 (H5'/H5")

NOEs involving the H5'/H5' and H4' protons were originally treated as $(\Sigma r^{-6})^{-1/6}$ sums between various possibilities, and ambiguities were subsequently resolved by an examination of the resulting ensemble of calculated structures. The same is true for NOEs involving T25 (CH$_3$) and T24 (H2') which have degenerate shifts.

both the 5' and 3' base pairs (Fig. 1). As is typically found in NMR spectra of DNA in solution, the base pairs at the end of the duplex fray, giving rise to extremely broad signals for base pairs 1, 2 and 17 which are only discernable in the 1D ^{1}H NMR spectrum of the complex. Thus, if the resonance at 12.33 ppm belonged to the DNA, it could only belong to one of the two unassigned imino positions at base pairs 6 or 7. Unfortunately, there were no unambiguous sequential assignments connecting either the imino proton of base pair 5 or the imino proton of base pair 8 to the signal at 12.33 ppm.

The original assignment of the resonance at 12.33 ppm to base pair 6 was based on reasoning which appeared to be consistent with previously published biochemical data (Werner et al., 1995b). First, binding site selection experiments for a number of ETS family members indicated that base pair 6 is virtually always a C•G base pair and this position is most commonly C•G in ETS binding sites identified for a large number of ETS-dependent enhancer sequences (Wasylyk et al., 1993). Second, hypersensitivity to DNase I cleavage had been observed for the anti-sense strand at base pair 7 for a number of ETS family members (Nye et al., 1992; Galson et al., 1993), suggesting a structural alteration or strain at this position in the complex; it was originally suggested that the DNA is kinked at this position (Werner et al., 1995b). Since NOEs to the

protein were only observed to one putative imino proton, we reasoned that the absence of NOEs to a second, neighboring imino proton must be due to some type of broadening mechanism. One broadening mechanism that is commonly observed for DNA imino protons is rapid exchange with the bulk solvent. Thus, it was inferred that the NOEs to the second imino proton were broadened away as a consequence of partial base pair disruption leading to rapid exchange of this proton with the bulk solvent. On the basis of this information, the resonance at 12.33 ppm was therefore assigned to belong to base pair 6, and base pair 7 was assumed to be partially disrupted in the complex.

In the light of the crystal structure of the Pu.1-DBD/DNA complex, the origin of the resonance at 12.33 ppm was reexamined spectroscopically. Two additional NMR experiments revealed unambiguously that this signal actually derives from the protein. First, a 3D ^{13}C-edited HMQC-NOESY spectrum recorded in H$_2$O, as opposed to the usual D$_2$O solvent normally used in this experiment, revealed two NOEs to the proton at 12.33 ppm: a strong NOE to the H$^\epsilon$ ring proton of Tyr[86] (6.99 ppm; ^{13}C$^\epsilon$ at 118.74 ppm) and a second, weaker NOE to the H$^{\delta 1}$ proton of Trp[28] (7.42 ppm; ^{13}C$^\delta$ at 127.7 ppm) (Fig. 2). Thus, the 3D ^{13}C-edited NOE spectrum in H$_2$O indicated that the proton giving rise to the signal at 12.33 ppm was close to Tyr[86]-H$^\epsilon$, raising the possibility that the signal at 12.33 ppm belonged to an as yet unassigned proton in the protein. In particular, the strength of the NOE to Tyr[86]-H$^\epsilon$ implied that the signal at 12.33 ppm might belong to the Tyr[86]-OH as the hydroxyl proton is only ~2.5 Å away from the Tyr[86]-H$^\epsilon$. Indeed, the observation of the strong NOE between Tyr[86]-H$^\epsilon$ and the resonance at 12.33 ppm in the 3D ^{13}C-edited NOE spectrum recorded in H$_2$O also revealed the misassignment of the Trp[28]-H$^{\delta 1}$ proton in the original paper (Werner et al., 1995b) since this resonance was thought to be degenerate with that of Tyr[86]-H$^\epsilon$. As a result, the cross peak in the 2D ^{1}H-^{1}H NOE spectrum recorded in H$_2$O between the resonances at 12.33 and 6.99 ppm was originally assigned to Trp[28]-H$^{\delta 1}$ in Fig. 1 of Werner et al. (1995b) but actually belongs to Tyr[86]-H$^\epsilon$.

If the signal at 12.33 ppm was the tyrosine hydroxyl proton, then it should show a weak ^{3}J coupling to the C$^\epsilon$ carbon of the tyrosine ring. A 1D heteronuclear spin-echo difference spectrum demonstrated (after about 20 h and 76 800 transients) that the signal at 12.33 ppm indeed was weakly coupled to ^{13}C (Fig. 2). On the basis of the integrated peak intensities in the heteronuclear difference experiment, we estimate the upper limit of this coupling to be ~6.5 Hz (if only one of the couplings is substantial). Since the signal at 12.33 ppm is weakly coupled to ^{13}C, it cannot arise from a DNA proton as the DNA was not ^{13}C-enriched. Therefore, the NOEs observed to the proton resonating at 12.33 ppm do not arise as a result of pro-

tein side-chain intercalation into the DNA. Hence, the interaction of the ETS1-DBD with DNA was grossly misinterpreted. Although we still have not been able to identify the imino proton resonances of base pairs 6 and 7, we hypothesize that they are either broadened beyond detection or unresolved from the group of G-imino resonances clustered between 12.7 and 12.9 ppm (Fig. 1).

Tyrosine hydroxyl protons have not been frequently reported in protein NMR spectra (see, for example, Kraulis et al. (1989), Torchia et al. (1989) and Liepinsh et al. (1992)). Ordinarily, hydroxyl protons exchange very rapidly with the solvent and are therefore not commonly observed in the ^{1}H NMR spectra of proteins. Indeed, in one case (Liepinsh et al., 1992), the hydroxyl proton could only be observed at low temperature (5 °C). In two other cases, tyrosine hydroxyl resonances were observed at 9.01 ppm (Kraulis et al., 1989) and 9.67 ppm (Torchia et al., 1989) at room temperature as a consequence of stable hydrogen bonding within the protein hydrophobic core. More recently, there have been three reports of the observation of a tyrosine hydroxyl proton downfield of 11 ppm. T4 lysozyme (McIntosh et al., 1990; Pjura et al., 1993), *Bacillus cirulans* xylanase (Plesniak et al., 1996) and Δ^5-3-ketosteroid isomerase (Zhao et al., 1996) possess broad, low-field resonances at 11.3, 11.5, 12.6 and 18.1 ppm, respectively. In each of these cases, the assignment as a Tyr-**OH** appears to have been made by inference either by examination of a crystal structure, by a process of elimination which includes the absence of an observable [1]H-^{15}N coupling, or by mutagenesis. The low-field frequency observed for the proton at 12.33 ppm and the fact that it was only observed in the complex were the primary factors which led us to an erroneous conclusion. It is interesting to note that this low-field resonance was readily observable in the complex at 32 °C but could not be observed in the free ETS1-DBD at any temperature, implying an unusually strong protection from exchange with the bulk solvent. In addition, the tyrosine hydroxyl resonance was observed neither in the free mouse ETS1-DBD nor in the free human Fli-1-DBD (L. McIntosh and S. Fesik, personal communication). Although two adjacent tyrosines, Tyr[85] and Tyr[87], are also buried at the interface in the ETS1-DBD/DNA complex, we can find no evidence for the protection of their hydroxyl protons from exchange with bulk solvent in the complex. The origin of the 2.5–3.5 ppm downfield shift of Tyr[86]-**OH** to 12.33 ppm in the present case may derive from a combination of hydrogen bonding to the phosphate backbone and a ring current shift from the neighboring Trp[28] (Fig. 4C).

Orientation of the ETS1-DBD on DNA

Defining the orientation of a protein domain on DNA requires the observation of a number of NOEs between DNA bases and protein side chains. Fifteen NOEs were

observed between the protein and the resonance at 12.33 ppm. The original assignment of these cross peaks as arising from intermolecular interactions with the DNA imino proton of G29 at base pair 6 anchored the protein to one end of the DNA duplex (Werner et al., 1995b). Therefore, the misassignment of these NOEs proved to be a devastating error. In the absence of the NOEs originally assigned to the imino proton of G29, the few base-specific NOEs observed were not sufficient to unambiguously define the orientation of the ETS1-DBD on the DNA. These base-specific NOEs, namely Lys[71] (H$^\epsilon$)→T25 (H6), Lys[78] (H$^\alpha$)→T25 (CH$_3$), Arg[81] (H$^\beta$)→T25 (H6) and Tyr[85] (H$^\epsilon$/H$^\delta$)→T24 (CH$_3$), involve residues of the major groove recognition helix (H3) interacting with the core GGAA motif in the center of the DNA duplex (Fig. 2 and Table 1). As these occur in the center of the DNA duplex, it was desirable to observe NOEs to amino acids in other regions of the protein as an independent check of the protein domain's polarity on the DNA. Unfortunately, all
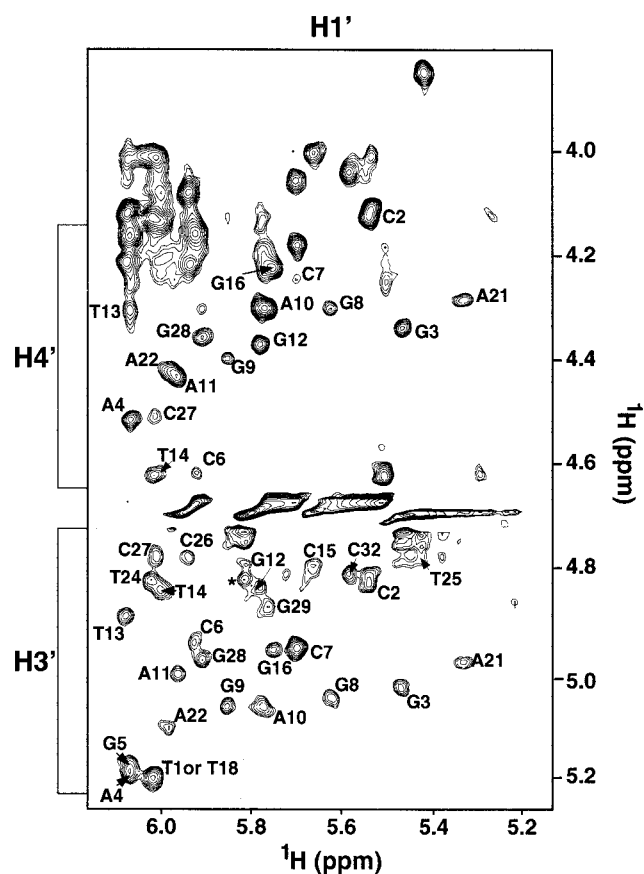

Fig. 3. Assignment of the H3' and H4' protons in the ETS1/DNA complex. A region of the ^{12}C-filtered [1]H-^{1}H NOESY spectrum recorded with a mixing time of 85 ms at 32 °C illustrates the extent of near-degeneracies for the chemical shifts of the H3' and H4' resonances in the ETS1/DNA complex. Labeled cross peaks represent the assignment of the H1'-H3' and H1'-H4' NOEs as indicated along each axis. Unlabeled cross peaks upfield of 4.4 ppm are the H5' and H5" cross peaks whose labels have been omitted for clarity. The asterisk indicates a cytosine H5-H3' NOE.

TABLE 2
STRUCTURAL STATISTICS[a]

	<SA>	$\overline{(SA)}$r
Rms deviations from experimental distance restraints (Å)[b]		
All (1619)	0.035 ± 0.002	0.037
Protein		
Interresidue sequential (|i–j| = 1) (255)	0.035 ± 0.007	0.029
Interresidue short range (1 < |i–j| ≤ 5) (160)	0.054 ± 0.008	0.071
Interresidue long range (|i–j| > 5) (267)	0.050 ± 0.006	0.052
Intraresidue (206)	0.008 ± 0.006	0.021
H-bonds (56)	0.039 ± 0.011	0.024
DNA		
Intraresidue (307)	0.015 ± 0.002	0.014
Sequential intrastrand (199)	0.019 ± 0.003	0.014
Interstrand (78)	0.024 ± 0.005	0.017
H-bonds (61)	0.022 ± 0.004	0.017
Protein/DNA (30)	0.069 ± 0.014	0.080
Rms deviations from experimental		
Dihedral restraints (°) (312)[b]	1.11 ± 0.04	1.16
$^3J_{HN\alpha}$ coupling constants (Hz) (49)[b]	0.90 ± 0.03	1.06
^{13}C shifts		
$^{13}C^\alpha$ (ppm) (78)	1.08 ± 0.05	1.07
$^{13}C^\beta$ (ppm) (55)	0.86 ± 0.05	0.88
Deviations from idealized covalent geometry		
Bonds (Å) (2776)	0.006 ± 0.0002	0.007
Angles (°) (5013)	1.033 ± 0.011	1.162
Impropers (°) (1469)	0.380 ± 0.030	0.664
E_{L-J} (kcal/mol)[c]	−878 ± 11	−765
Coordinate precision[d]		
Protein backbone + DNA	1.02 ± 0.16	
All protein atoms + DNA	1.28 ± 0.13	
Protein backbone	0.73 ± 0.10	
All protein atoms	1.29 ± 0.12	
DNA	0.88 ± 0.16	

[a] The notation of the NMR structures is as follows: <SA> – final 25 simulated annealing structures; $\overline{SA}$ – mean structure obtained by averaging the coordinates of the individual SA structures best fitted to each other (with respect to residues 24–105 of the protein and base pairs 1–17 of the DNA); $\overline{(SA)}$r – restrained regularized mean structure obtained by restrained regularization of the mean structure $\overline{SA}$. The number of terms for the various restraints is given in parentheses. Note that as residues 1–9 are completely disordered in solution, the experimental restraints for the protein relate to residues 10–105.

[b] None of the structures exhibited distance violations greater than 0.5 Å, dihedral angle violations greater than 10° or $^3J_{HN\alpha}$ coupling constant violations greater than 2 Hz. There are 196 torsion angle restraints for the DNA (α, β, γ, δ, ε and ζ angles; Werner et al., 1995b) and 116 for the protein (88 φ, 2 ψ, 12 χ_1 and 14 aromatic χ_2 angles).

[c] E_{L-J} is the Lennard-Jones van der Waals energy calculated with the CHARMM PARAM19/20 protein and PARNAH1ER1 DNA parameters (Brooks et al., 1983) and is *not* included in the target function for simulated annealing or restrained regularization.

[d] The precision of the coordinates is defined as the average atomic rms difference between the 25 individual simulated annealing structures and the mean coordinates $\overline{SA}$. The values refer to residues 24–105 of the protein and base pairs 1–17 of the DNA. The first 23 residues of the protein are disordered in solution.

the other intermolecular NOEs originally assigned involved the H3', H4', H5' and H5" sugar resonances of the DNA which are considerably overlapped and can only be assigned in the 3D ^{13}C-separated/^{12}C-filtered NOE spectrum by reference to the 2D ^{12}C-filtered NOE spectrum of the complex (Fig. 3). Thus, while we were often able to narrow down the assignment of these intermolecular NOEs to sugar protons as belonging to one of two or three residues in the DNA sequence, the ultimate assignment of these NOEs relied on early structural models of the complex generated on the basis of the misassigned intermolec-

ular NOEs involving the imino proton of G29. Therefore, a large number of the interfacial NOEs, about half of those originally reported, were erroneously assigned on the basis of an incorrect model of the interaction between protein and DNA. New information derived from a fresh sample recorded at 600 MHz revealed several new NOEs between Met[74] and T25, and between Tyr[76], Arg[99] and Tyr[100] and the sugar protons of G5 (Fig. 2 and Table 1). Combined with the reassignment of the NOEs to the resonance at 12.33 ppm, the orientation of the ETS1-DBD on DNA has to be reversed relative to that orig-

inally reported (Werner et al., 1995b) and is consistent with the orientation of the Pu.1-DBD on the Pu.1 operator sequence (Kodandapani et al., 1996). The location, however, of the recognition helix H3 of the HTH motif in the major groove is unchanged (Werner et al., 1995b), except that it runs in the opposite direction.

Structure determination of the ETS1-DBD/DNA complex

The corrected solution structure of the ETS1-DBD/DNA complex was derived from multidimensional heteronuclear-filtered and -edited NMR experiments (Gronenborn and Clore, 1995) and was based on 2113 experimental NMR restraints. A summary of the structural statistics is given in Table 2. A superposition of the final 25 simulated annealing (SA) structures is shown in Fig. 4A and a ribbon diagram of the restrained regularized mean structure is shown in Fig. 4B. The precision of the coordinates for the protein backbone (residues 24–105) and the DNA (base pairs 1–17) is ~1 Å. Residues 1–23 are poorly defined by the data.

Overall, the architecture and topology of the ETS1-DBD remain essentially unchanged relative to the structure of the DBD reported earlier (Werner et al., 1995b). There are a few local changes in the packing arrangement, most notable of which is an ~20° rotation in the orientation of helix H1 relative to its position in the original
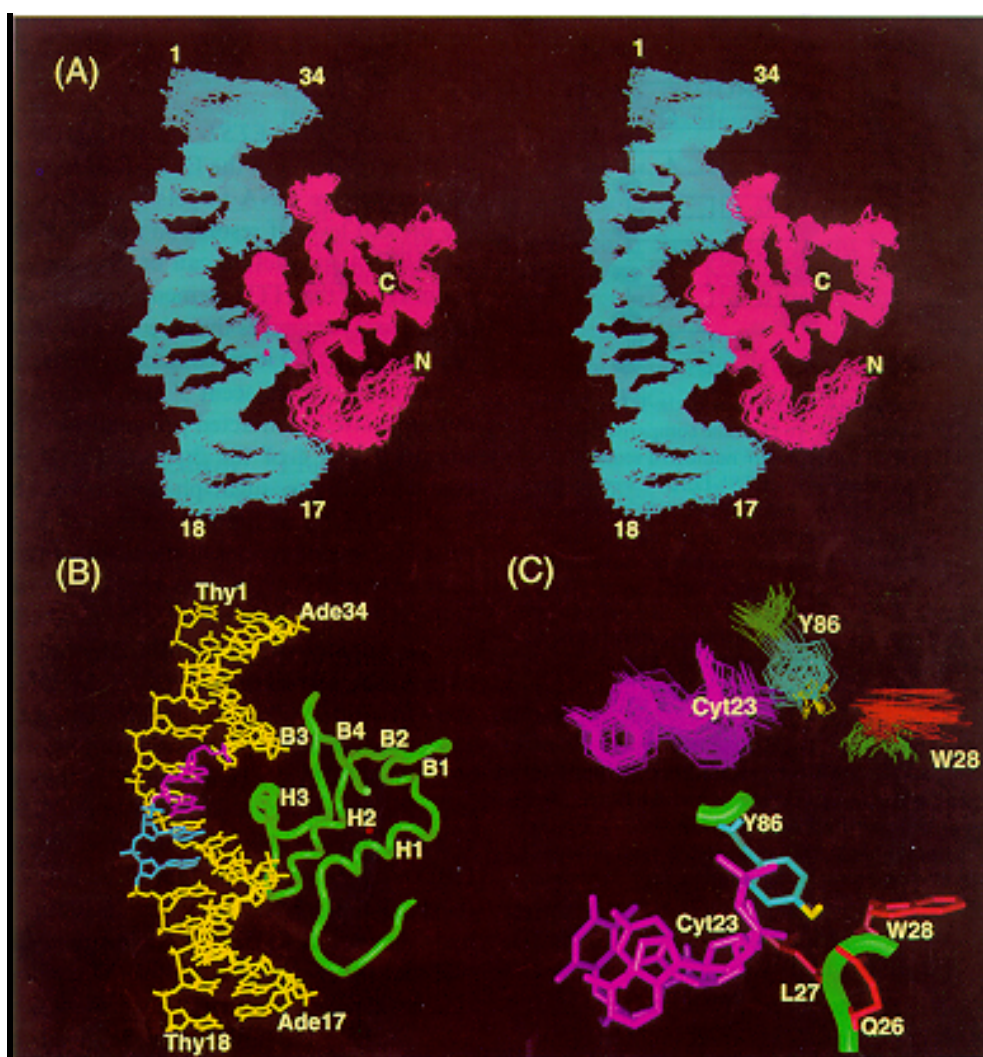

Fig. 4. Corrected solution structure of the ETS1-DBD/DNA complex. (A) Stereoview showing a best-fit superposition of the final 25 simulated annealing structures of the ETS1-DBD/DNA complex, with the backbone of the ETS1-DBD in red and the DNA 17-mer in blue (residues 17–105 of the protein are shown, since residues 1–23 are poorly defined by the NMR data). (B) The interaction of the ETS1-DBD with the DNA includes amino acids from helix H3 in the major groove and amino acids in the loop between β-strands B3 and B4 as well as the loop between helices H2 and H3. The protein is shown as a tube in green; the DNA is shown in yellow with the central GGAA motif in magenta for guanine residues and in blue for adenine residues. (C) Detailed view illustrating the position of the hydroxyl proton (yellow) of Tyr[86] (blue) with respect to the DNA (purple) and the ring of Trp[28] (red). The superposition of the final 25 simulated annealing structures is shown for Trp[28] and Tyr[86] of the ETS1-DBD and A22 and C23 of the DNA. The minimized averaged structure is also shown, indicating the approximate orientation of the Tyr[86]-OH in yellow. The side chains of Gln[26] (red) and Leu[27] (red) form the balance of a cluster of amino acids in this region of the DNA, near C23. This figure was prepared with the program GRASP (Nicholls et al., 1991).
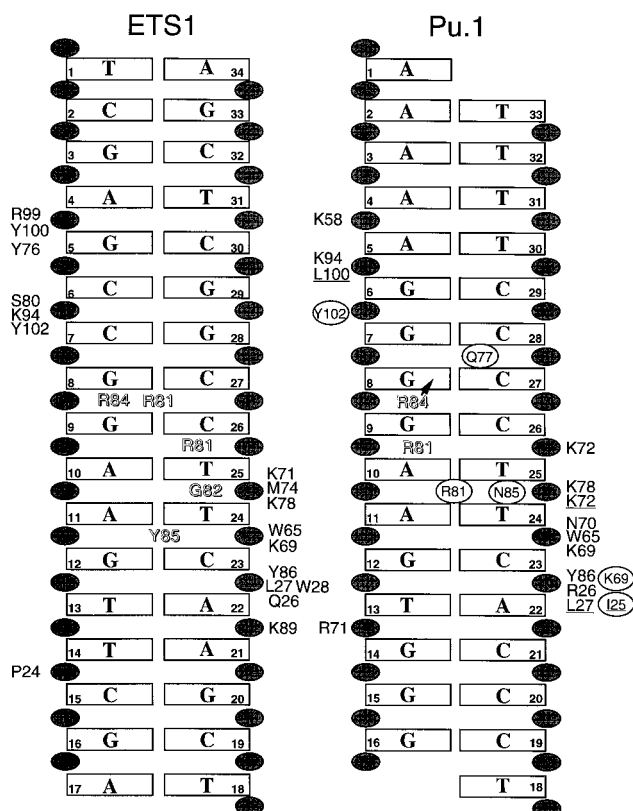
Fig. 5. Summary of the protein/DNA interactions in the ETS1-DBD/DNA and Pu.1-DBD/DNA complexes. To facilitate comparison to the ETS1-DBD, amino acids in the Pu.1-DBD are numbered sequentially using the generic numbering scheme of the ETS1-DBD. Likewise, the numbering of the DNA bases for the Pu.1-DBD/DNA complex is according to the ETS1 17-mer DNA employed in the current study. Shaded ellipses represent the sugar-phosphate backbone; boxes indicate the DNA bases. Amino acids next to ellipses form contacts with either the sugar or phosphate for that residue. Encircled amino acids represent water-mediated contacts observed in the Pu.1-DBD/DNA crystal structure (Kodandapani et al., 1996). Underlined amino acids indicate contacts with the protein backbone for that residue. Open boxed letters indicate residues that form direct contacts with the DNA bases. The contacts for Gln[26], Trp[28], Gly[82], Arg[84] and Tyr[102] are inferred from the structure and have not been identified on the basis of observed NOEs between these protein side chains and the DNA. The putative hydrogen bond between Trp[65] and the phosphate of T24 is inferred from the 1.5 ppm downfield shift in the indole proton resonance upon complexation. Numerous NOEs position Trp[65] in such a way as to make the phosphate of T24 the only logical hydrogen-bond acceptor.

structure. This is a consequence of nearly 20 medium and strong NOEs that were previously assigned to interaction with the DNA that have now been correctly assigned to involve close contacts with Tyr[86]. As helix H1 is located at the N-terminus of the protein, it is not surprising that the correction of these NOEs has altered the position of helix H1 slightly. In addition, since Trp[28] no longer intercalates into the DNA and since the DNA is no longer located between helix H3 and the N-terminal end of helix H1, the DBD is packed more tightly than in the original structure. Finally, contacts between the 'wing' formed by

the loop between strands 3 and 4 and the DNA impart a modest twist in these two strands of β-sheet.

Similarly, with the evident exception of the ~60° kink between base pairs 6 and 7 in the incorrect structure of the complex (Werner et al., 1995b), the conformation of the DNA also remains essentially unaltered. Thus, the rms difference between the DNA coordinates of the correct and incorrect structures is 3.9 Å for base pairs 1–17, but only 0.8 Å for base pairs 1–6 and 1.4 Å for base pairs 7–17.

A detailed view of the environment of the hydroxyl proton of Tyr[86] is shown in Fig. 4C for the 25 SA structures. It can be seen that the hydroxyl proton of Tyr[86] (yellow) lies in the plane of the ring of Trp[28] and may be hydrogen-bonded to the phosphate of C23, possibly accounting for its substantial downfield shift in the ^{1}H NMR spectrum.

Comparison of the ETS1- and Pu.1-DBD/DNA complexes

The interaction of the ETS1-DBD and Pu.1-DBD with their respective DNA targets is very similar, although at the present level of resolution not all of the details of the ETS1/DNA interaction can be discerned (Figs. 4 and 5). Helix H3 of the HTH element is positioned in the major groove and recognizes the core GGAA motif. Two regions of the ETS1-DBD form contacts with the sugar-phosphate backbone at the adjacent 5' and 3' minor grooves. The 5' minor groove is contacted principally by the loop between strands 3 and 4 of the β-sheet. The 3' minor groove is contacted at the sugar-phosphate backbone by Gln[26], Leu[27] and Trp[28] at the N-terminus of helix H1, Trp[65] of helix H2, several lysines in the turn between helix H2 and helix H3, and Tyr[86] of helix H3. The indole NH of Trp[65] and the hydroxyl proton of Tyr[86] are closely positioned to the phosphates of T24 and C23, respectively, and are likely to be hydrogen-bonded to the DNA backbone at these positions. This would account for the downfield shifted resonances of these two protons. Further, the postulated hydrogen bond involving the hydroxyl of Tyr[86] would account for its presence in the complex at 32 °C, and its complete absence in the free, uncomplexed ETS1-DBD. A very similar pattern of contacts is observed for the Pu.1-DBD/DNA complex, including intermolecular hydrogen bonds to the DNA phosphates from the indole NH and the hydroxyl group of the tryptophan and tyrosine residues, respectively, corresponding to Trp[65] and Tyr[86] of the ETS1-DBD (Fig. 5). A more detailed comparison is not possible at the present time since the coordinates of the Pu.1-DBD/DNA complex were not made available to us.

Discussion and Conclusions

Structure determination

The occurrence of the Tyr[86]-**OH** resonance in a region of the ^{1}H NMR spectrum where ordinarily only DNA

imino proton resonances are found led to the crucial misassignment which resulted in the incorrect orientation of the ETS1-DBD on DNA. If this resonance had been observed in the free ETS1-DBD, the original assignment of this resonance as a DNA imino proton would not have been made. Confounding the analysis in this case was the difficulty in making unambiguous assignments for many of the intermolecular NOEs to the H3', H4', H5' and H5" sugar protons of the DNA. These protons appear in a crowded region of the spectrum and while many can be assigned, there are near-degeneracies for several H3' and H4' protons and many complete degeneracies for the H5' and H5" protons. In the ETS1-DBD/DNA complex, about 90% of the intermolecular restraints involved these sugar protons, thereby precluding a model-independent assignment for the bulk of intermolecular contacts. It was unusual that NOEs were only observed to one putative imino proton instead of two and this should have been viewed as highly suspicious. The experiments reported in this paper, which ultimately demonstrated that the resonance at 12.33 ppm does not arise from a DNA imino proton, should have been considered from the outset as a check on the original interpretation of the data. With hindsight it is clear that we exercised poor judgement in assessing the origin of the signal at 12.33 ppm – indeed chemical shift reasoning alone has a history of leading one astray.

The orientation of the protein domain in the present model is derived from two distinct regions of the protein, helix H3 which interacts in the major groove with the core GGAA recognition motif and the 'wing' formed by the loop between β-strands 3 and 4 interacting with the sugar-phosphate backbone of G5 in the 5' half of the DNA duplex. These observations, coupled with the corrected assignments discussed above, appear to define a unique orientation of the protein domain on the DNA. An independent analysis of the ETS1/DNA and Pu.1/DNA interactions using chemical footprinting by Graves et al. (1996) is consistent with the revised structure reported here and with the X-ray structure of the Pu.1/DNA complex (Kodandapani et al., 1996). Given our recent experience, we have not attempted to complete any model-based assignments of the intermolecular NOEs to the sugar protons which are obscured by inadequate spectral resolution. Thus, the present model is based on approximately one-half the number of intermolecular restraints (Table 1) as compared to our original report (Werner et al., 1995b).

One may wonder why we failed to see NOE violations in calculating the original model of the ETS1/DNA interaction. This is due to the fact that the errors in NOE assignments occurred at the interface between protein and DNA and not in either of the NOE sets defining the structure of either component of the complex. These assignment errors were self-consistent and therefore could not lead to unresolved NOE violations during structure refinement. It is expected that, in most cases, conflicting

assignments at the interface, such as NOEs to regions of protein on opposite sides of the molecule, will reveal a set of crucial misassignments during the interfacial NOE analysis. However, when there is ambiguity in the assignment of many NOEs, as seen in this case with the interfacial NOEs to H4', H5' and H5" sugar protons, there is a need for independent verification of the model even if it comes from data derived from other methods. We have since pursued such studies, including mutagenesis of Trp[28] (to Ala) and alteration of the DNA sequence at base pairs 6 and 7. In both cases, DNA binding was abolished, consistent with the original conclusion that this region of the DNA and this amino acid in the protein play an important role in the interaction (data not shown). As evidenced by our own spectroscopy studies, this role, however, does not involve side-chain intercalation. Future structural efforts need to eliminate the reliance on a model for the interpretation of the interfacial NOE assignments in cases such as the present one. Clearly, had we been able to uniformly enrich the DNA with ^{13}C and ^{15}N, we would never have concluded that the resonance at 12.33 ppm was an imino proton. Moreover, isotopic enrichment would have likely permitted us to resolve many of the near-degeneracies in the sugar protons which comprised the bulk of intermolecular contacts between protein and DNA.

Although many details of the ETS1/DNA interaction were readily identified from the NMR study, some important aspects remain unclear. The main drawback of the present study in solution concerns the orientation of the functional groups of the highly conserved Arg[81] and Arg[84] residues with respect to the DNA. Significant line broadening in the complex precluded complete assignment for several lysine and arginine residues in the HTH motif of the ETS1-DBD. As a consequence, only a few contacts were observed between the Arg[81] side chain, none beyond C^β, and no direct contacts were observed between the Arg[84] side chain and the DNA. The positions of these residues are largely determined by the NOEs to other protein side chains. It was observed spectroscopically that all of the arginine $N^\epsilon H$ and some of the arginine guanidino protons were protected from rapid exchange with bulk solvent in the ETS1-DBD/DNA complex. Very few of these exchangeable protons, however, could be sequence-specifically assigned, particularly because the C^δ (arginine) or C^ϵ (lysine) positions could not be unambiguously identified for every lysine or arginine residue in the protein domain. As a result, the orientations of the Arg[81] and Arg[84] side chains are underdetermined in the present NMR structure of the ETS1-DBD/DNA complex.

Acknowledgements

References

Blake, P.R., Lee, B., Summers, M.F., Adams, M.W.W., Park, J.-B., Zhou, Z.H. and Bax, A. (1992) *J. Biomol. NMR*, **2**, 527–533.

Brooks, B.R., Bruccoleri, R.E., Olafson, B.D., States, D.J., Swaminathan, S. and Karplus, M. (1983) *J. Comput. Chem.*, **4**, 187–217.

Brünger, A.T. (1993) *XPLOR Manual Version 3.1*, Yale University, New Haven, CT, U.S.A.

Delaglio, F., Grzesiek, S., Vuister, G.W., Zhu, G., Pfeifer, J. and Bax, A. (1995) *J. Biomol. NMR*, **6**, 277–293.

Donaldson, L.W., Petersen, J.M., Graves, B.J. and McIntosh, L.P. (1994) *Biochemistry*, **33**, 13509–13516.

Donaldson, L.W., Petersen, J.M., Graves, B.J. and McIntosh, L.P. (1996) *EMBO J.*, **15**, 125–134.

Fisher, R.J., Mavrothalassitis, G., Kondoh, A. and Papas, T.S. (1991) *Oncogene*, **6**, 2249–2254.

Fisher, R.J., Fivash, M., Casas-Finet, J., Erickson, J.W., Kondoh, A., Bladen, S.V., Fisher, C., Watson, D.K. and Papas, T. (1994) *Protein Sci.*, **3**, 257–266.

Galson, D.L. and Housman, D.E. (1988) *Mol. Cell. Biol.*, **8**, 381–392.

Galson, D.L., Hensold, J.O., Bishop, T.R., Schalling, M., D'Andrea, A.D., Jones, C., Auron, P.E. and Housman, D.E. (1993) *Mol. Cell. Biol.*, **13**, 2929–2941.

Garrett, D.S., Powers, R., Gronenborn, A.M. and Clore, G.M. (1991) *J. Magn. Reson.*, **95**, 214–220.

Garrett, D.S., Kuszewski, J., Hancock, T., Lodi, P.J., Vuister, G.W., Gronenborn, A.M. and Clore, G.M. (1994) *J. Magn. Reson.*, **B104**, 99–103.

Graves, B.J., Gillespie, M.E. and McIntosh, L.P. (1996) *Nature*, **384**, 322.

Gronenborn, A.M. and Clore, G.M. (1995) *Crit. Rev. Biochem. Mol. Biol.*, **30**, 351–385.

Hromas, R. and Klemsz, M. (1994) *Int. J. Hematol.*, **59**, 257–265.

King, C.-Y. and Weiss, M.A. (1993) *Proc. Natl. Acad. Sci. USA*, **90**, 11990–11994.

Kodandapani, R., Pio, F., Ni, C.Z., Piccialli, G., Klemsz, M., McKercher, S., Maki, R.A. and Ely, K.R. (1996) *Nature*, **380**, 456–460.

Kraulis, P.J., Clore, G.M., Nilges, M., Jones, T.A., Pettersson, G., Knowles, J. and Gronenborn, A.M. (1989) *Biochemistry*, **28**, 7241–7257.

Kuszewski, J., Qin, J., Gronenborn, A.M. and Clore, G.M. (1995) *J. Magn. Reson.*, **B106**, 92–96.

Lewis, M., Chang, G., Horton, N.C., Kercher, M.A., Pace, H.C., Schumacher, M.A., Brennan, R.G. and Lu, P. (1996) *Science*, **271**, 1247–1251.

Liang, H., Mao, X., Olejniczak, E.T., Nettesheim, D.G., Yu, L., Meadows, R.P., Thompson, C.B. and Fesik, S.W. (1994a) *Nat. Struct. Biol.*, **1**, 871–876.

Liang, H., Olejniczak, E.T., Mao, X., Nettesheim, D.G., Yu, L., Thompson, C.B. and Fesik, S.W. (1994b) *Proc. Natl. Acad. Sci. USA*, **91**, 11655–11659.

Liepinsh, E., Otting, G. and Wüthrich, K. (1992) *J. Biomol. NMR*, **2**, 447–465.

Love, J.J., Li, X., Case, D.A., Giese, K., Grosschedl, R. and Wright, P.E. (1995) *Nature*, **376**, 791–795.

MacLeod, K., Leprince, D. and Stehelin, D. (1992) *Trends Biochem. Sci.*, **17**, 251–256.

McIntosh, L.P., Wand, A.J., Lowry, D.F., Redfield, A.G. and Dahlquist, F.W. (1990) *Biochemistry*, **29**, 6341–6362.

Morris, A.L., MacArthur, M.W., Hutchinson, E.G. and Thornton, A.M. (1992) *Proteins Struct. Funct. Genet.*, **78**, 1595–1620.

Nicholls, A.J., Sharp, K.A. and Honig, B. (1991) *Proteins Struct. Funct. Genet.*, **11**, 281–296.

Nilges, M., Clore, G.M. and Gronenborn, A.M. (1988) *FEBS Lett.*, **229**, 129–136.

Nilges, M. (1993) *Proteins Struct. Funct. Genet.*, **17**, 295–309.

Nye, J.A., Peterson, J.M., Gunther, C.V., Jonsen, M.D. and Graves, B.J. (1992) *Genes Dev.*, **6**, 975–990.

Petersen, J.M., Skalicky, J., Donaldson, L.W., McIntosh, L.P., Alber, T. and Graves, B.J. (1995) *Science*, **269**, 1866–1869.

Pjura, P., McIntosh, L.P., Wozniak, J.A. and Matthews, B.W. (1993) *Proteins Struct. Funct. Genet.*, **15**, 401–412.

Plateau, P. and Guéron, M. (1982) *J. Am. Chem. Soc.*, **104**, 7310–7311.

Plesniak, L.A., Connelly, G.P., Wakarchuk, W.W. and McIntosh, L.P. (1996) *Protein Sci.*, **5**, 2319–2328.

Ray-Gallet, D., Mao, C., Tavitian, A. and Moreau-Gachelin, F. (1995) *Oncogene*, **11**, 303–313.

Rice, P.A., Yang, S.-W., Mizuuchi, K. and Nash, H.A. (1996) *Cell*, **87**, 1295–1306.

Shore, P. and Sharrocks, A.D. (1995) *Nucleic Acids Res.*, **23**, 4698–4706.

Torchia, D., Sparks, S.W. and Bax, A. (1989) *Biochemistry*, **28**, 5509–5524.

Voso, M.T., Burn, T.C., Wulf, G., Lim, B., Leone, G. and Tenen, D.G. (1994) *Proc. Natl. Acad. Sci. USA*, **91**, 7932–7936.

Wasylyk, B., Hahn, S.L. and Giovane, A. (1993) *Eur. J. Biochem.*, **211**, 7–18.

Werner, M.H., Clore, G.M., Gronenborn, A.M., Kondoh, A. and Fisher, R. (1994) *FEBS Lett.*, **345**, 125–130.

Werner, M.H., Bianchi, M.E., Gronenborn, A.M. and Clore, G.M. (1995a) *Biochemistry*, **34**, 11998–12004.

Werner, M.H., Clore, G.M., Fisher, C.L., Fisher, R.J., Trinh, L., Shiloach, J. and Gronenborn, A.M. (1995b) *Cell*, **83**, 761–771.

Werner, M.H., Huth, J.R., Gronenborn, A.M. and Clore, G.M. (1995c) *Cell*, **81**, 705–714.

Werner, M.H., Clore, G.M., Fisher, C.L., Fisher, R.J., Trinh, L., Shiloach, J. and Gronenborn, A.M. (1996a) *Cell*, **87**, issue 2.

Werner, M.H., Gronenborn, A.M. and Clore, G.M. (1996b) *Science*, **271**, 778–784.

Zhao, Q., Abeygunawardana, C., Talalay, P. and Mildvan, A.S. (1996) *Proc. Natl. Acad. Sci. USA*, **93**, 8220–8224.